ELSEVIER

Polymer 41 (2000) 5485–5503

polymer

Thermal and crystallisation behaviour of isotactic polypropylene/nitrile rubber blends

S. George[a], K.T. Varughese[b], S. Thomas[a,*]

[a]*School of Chemical Sciences, Mahatma Gandhi University, Priyadarshihi Hills P.O., Kottayam 686 560, Kerala, India*
[b]*Polymer Laboratory, CPRI, Bangalore 560 094, India*

Received 27 October 1998; received in revised form 2 March 1999; accepted 29 September 1999

Abstract

The thermal stability of isotactic polypropylene (PP)/nitrile rubber (NBR) was studied using thermogravimetry. The effects of blend ratio, compatibilisation and dynamic vulcanisation on thermal stability were investigated. The addition of nitrile rubber to polypropylene was found to improve the thermal stability of polypropylene. The compatibilisation of the blends using phenolic modified polypropylene and maleic anhydride modified propylene has increased the degradation temperature and decreased the weight loss. The dynamic vulcanisation of the blends also improved the thermal stability. The melting behaviour was investigated by differential scanning calorimetry for the binary blends. The crystallinity of the blends decreased with increase in NBR content. The crystalline structure of the blends was investigated using wide angle X-ray scattering. The polypropylene and the blends exist in the α-monoclinic form as shown by the presence of four maximas. The compatibilisation of the blends did not affect the α-monoclinic crystalline structure. The addition of NBR to polypropylene increased the interplanar distance.

Keywords: Polypropylene; Nitrile rubber; Compatibilisation

1. Introduction

Recently, the commercial importance of polymer blends are increasing high since the performance of polymers can improve by simple blending in order to fulfil industry's need for high performance materials. However, many of these high molecular weight polymers are immiscible and incompatible which lead to poor final properties [1,2]. Compatibilisation by the in situ formation of an interfacial agent and dynamic vulcanisation, i.e. vulcanisation of rubber phase in blends during mixing, of polymer blends were found to improve the properties of immiscible polymer blends by providing stable morphology, and good interfacial adhesion [3–6].

In order to develop durable industrial products it is necessary to investigate the thermal stability of these blends. Thermogravimetric analysis can be used as a way to measure the thermal stability of polymer due to the simplicity of this weight loss method [7,8]. The thermal degradation of polymer blends was investigated by various researchers using the thermogravimetric method [9,15]. The blending of a polymer with other polymers has stabilising as well as destabilising effects. Grassie et al. [9] reviewed these stabilising effects of blending. The complete degradation of PMMA into monomers on heating can be considerably reduced by blending with other polymers. The destabilising effect of PVC on the degradation of polymers was also investigated. Varughese et al. [10] reported that, the blending of ENR with PVC reduced the rate of HCl elimination in the first degradation step of PVC. The thermal degradation behaviour of blends has been used to identify SBR/BR blends from SBR based compounds by Amraee et al. [11] from the ratio of the peak heights of DTG peaks. The effect of miscibility of polymer blends on thermal degradation behaviour was investigated by Lizymol et al. [12] Among the different blends studied PVC/EVA, EVA/SAN and PVC/SAN, the thermal stability was improved in the

* Corresponding author. Tel: 91-481-598303; fax: 91-481-561190.
E-mail address: mgu@md2.vsnl.net.in (S. Thomas).

Abbreviations: BR: butyl rubber; BS: butadiene styrene rubber; DSC: differential scanning calorimetry; DTG: differential thermogravimetry; ENR: epoxidised natural rubber; EPDM: ethylene propylene diene monomer rubber; EVA: poly(styrene-*co*-vinyl acetate); HIS: hydrogenated butadiene styrene rubber; IR: infrared spectroscopy; LDPE: low density polyethylene; MA-PP: maleic anhydride modified polypropylene; NBR: nitrile rubber; NR: natural rubber; PA-6: Polyamide-6; PDMS: polydimethyl siloxane rubber; Ph-PP, phenolic modified polypropylene; PMMA: poly(methyl methacrylate); PP: polypropylene; PVC: polyvinyl chloride; SAN: styrene-*co*-acrylonitrile; SBR, styrene-*co*-butadiene rubber; SEBS: poly[styrene-b-(ethylene-*co*-butylene)-b-styrene]; TGA: thermogravimetry analyser; WAXS: wide angle X-ray scattering

0032-3861/00/$ - see front matter
PII: S0032-3861(99)00719-3

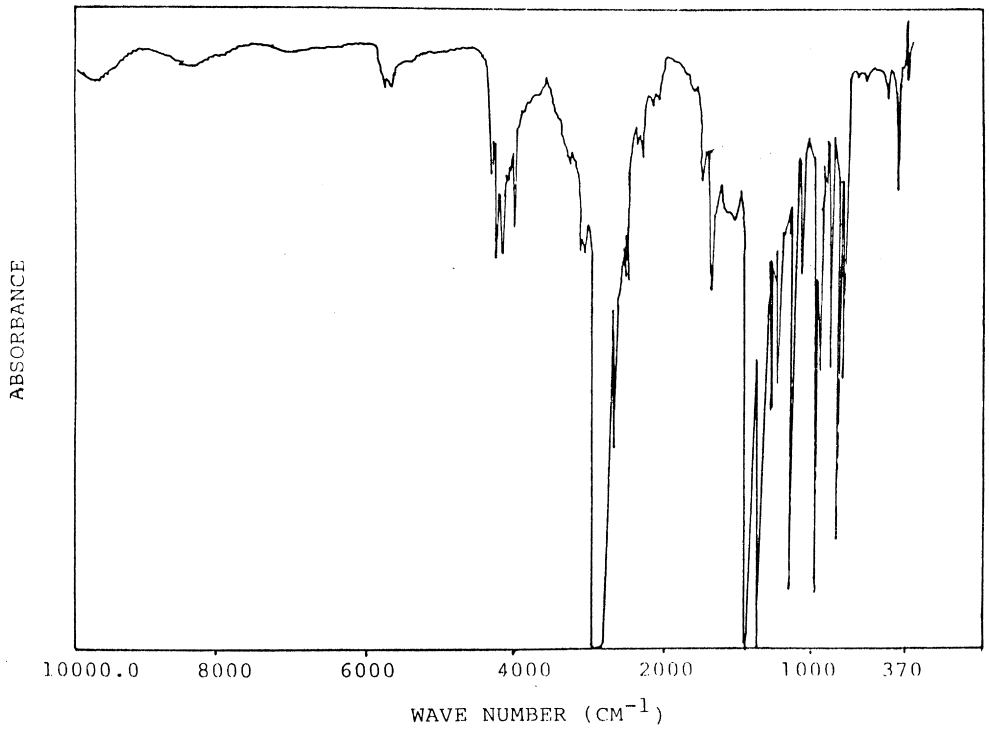

Fig. 1. IR spectrum of maleic anhydride modified PP.

case of miscible PVC/EVA system. In immiscible EVA/SAN and PVC/SAN blends there was not much improvement of thermal stability as a result of blending. Subhra et al. [13] reported that blends of ENR with poly(ethylene-*co*-acrylic acid) showed the existence of single phase at low concentrations of ENR, i.e. at 10, 20 and 30 wt%, as shown by the two-step degradation that exist in these blends.

In polymer blends with a crystallisable component, the final properties are determined by: (1) mode and state of dispersion of rubbery domains in the crystalline matrix; (2) the texture, dimensions and size distribution of spherulites of the matrix; (3) the inner structure of spherulites, i.e. lamellar and inter lamellar thickness; (4) physical structure of inter spherulitic boundary regions and amorphous inter lamellar regions; and (5) the adhesion between the rubbery domains and the crystalline matrix [14–17]. The effect of the nature of crystalline structure and the extent of crystallinity on the properties of various polymer blends was investigated [18–28]. Martuscelli et al. [18,19] investigated the nucleation and growth of spherulites in various rubber/plastic blends. Hlavata et al. [20] investigated the change in crystalline structure of iPP on blending with two thermoplastic elastomers, butadiene–styrene (BS) and hydrogenated butadiene styrene rubbers (HIS). The pure polypropylene and blends with BS and HIS showed the presence of hexagonal β phase along with the α-form. The thermal and crystallisation behaviour of EVA/NR blends was investigated by Koshy et al. [21] The crystallinity of the blends decreased with increase in NR content, and the interplanar distance *d* values increased on the addition of NR indicating the migration of NR phase into the interchain space of EVA.

The effect of compatibilisation on the crystallisation behaviour was studied by Santra et al. [22]. They reported that the crystallinity of LDPE/PDMS rubber blends increased upon compatibilisation using ethylene methyl acrylate copolymer. Wu et al. reported that in PA-6/SEBS blends [23], the compatibilisation using maleated SEBS changes the α-crystalline form of PA-6 in binary blends to a mixture of α- and γ-crystalline forms. The effect of dynamic vulcanisation on crystallinity and crystalline structure was reported for dynamic vulcanised PP/EPDM blend [24,25].

Blends of polypropylene with nitrile rubber possess the excellent processing characteristics and mechanical properties of polypropylene with the oil resistance and flexibility of NBR. However, these blends are incompatible and require compatibilisation for better properties [29]. In this

Table 1
Formulation of dynamic vulcanised blends

	PS	PC	PM
PP	70	70	70
NBR	30	30	30
Sulphur	2	–	0.1
DCP[a]	–	2	1
TMTD[b]	2.5	–	2.5
CBS[c]	2	–	2
ZnO	5	–	5
St. acid	2	–	2

[a] Dicumyl peroxide.
[b] Tetramethyl thiuram disulphide.
[c] *N*-Cyclohexyl benzothiazyl sulphenamide.

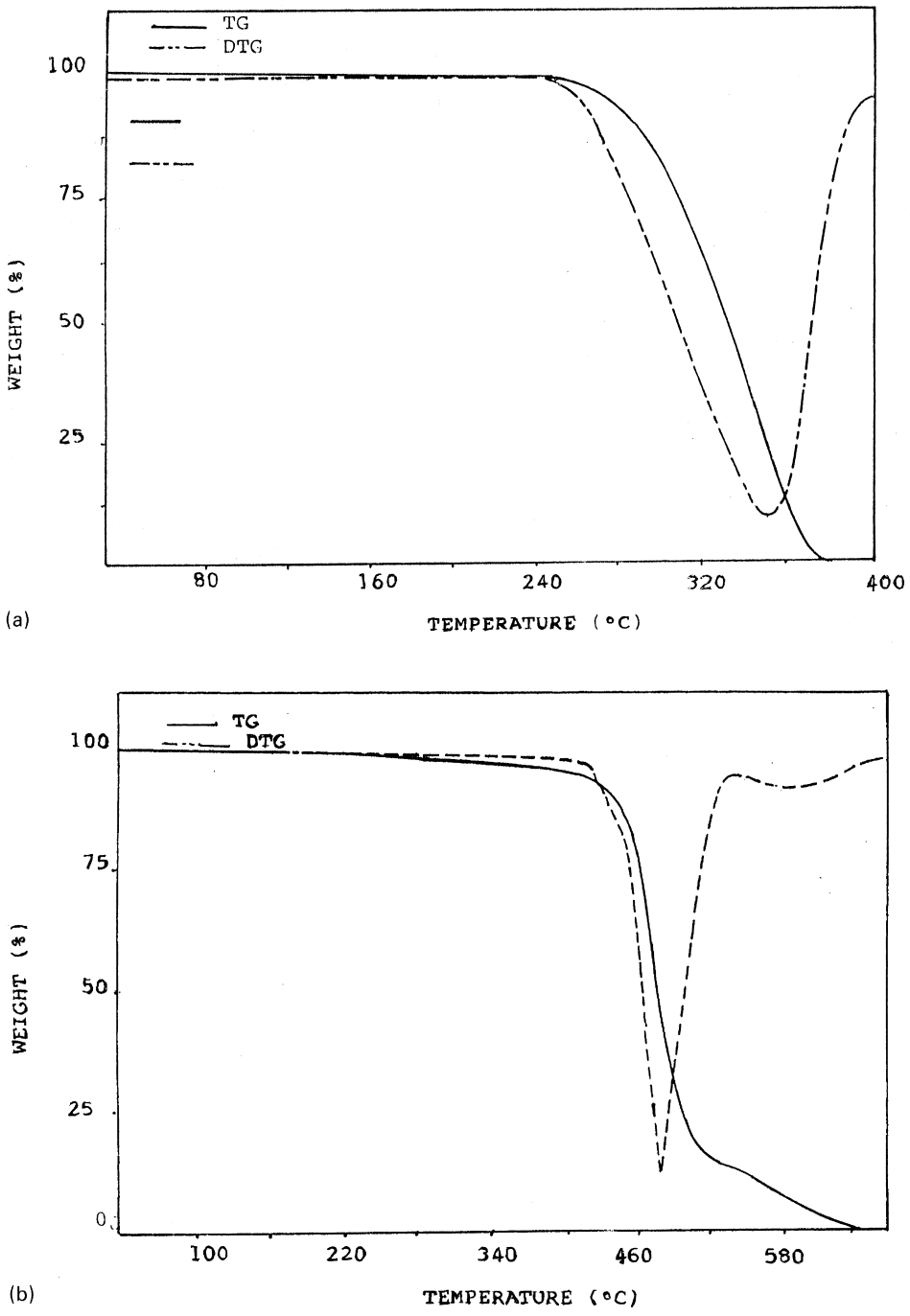

Fig. 2. Thermograms and derivative thermograms of PP/NBR blends: (a) P_{100}; (b) P_{70}; (c) P_{50}; (d) P_{30}; and (c) P_0.

laboratory, we have investigated the effect of compatibilisation and dynamic vulcanisation on morphology and various properties [30–32]. However, no attempts have been made so far to investigate the thermal and crystallisation behaviour of PP/NBR blends. In this paper, we have studied the thermal properties of uncompatibilised, reactively compatibilised and dynamic vulcanised PP/NBR blends. The crystalline structure of both uncompatibilised and compatibilised blends was also investigated.

2. Experimental

2.1. Materials

Isotactic polypropylene (Koylene M3060) having an MFI of 3 g min^{-10} was supplied by IPCL, Baroda. Acrylonitrile *co*-butadiene rubber (Chemaprene N3309) with an acrylonitrile content of 34% was supplied by Synthetics and Chemicals, Bareli, UP, India.

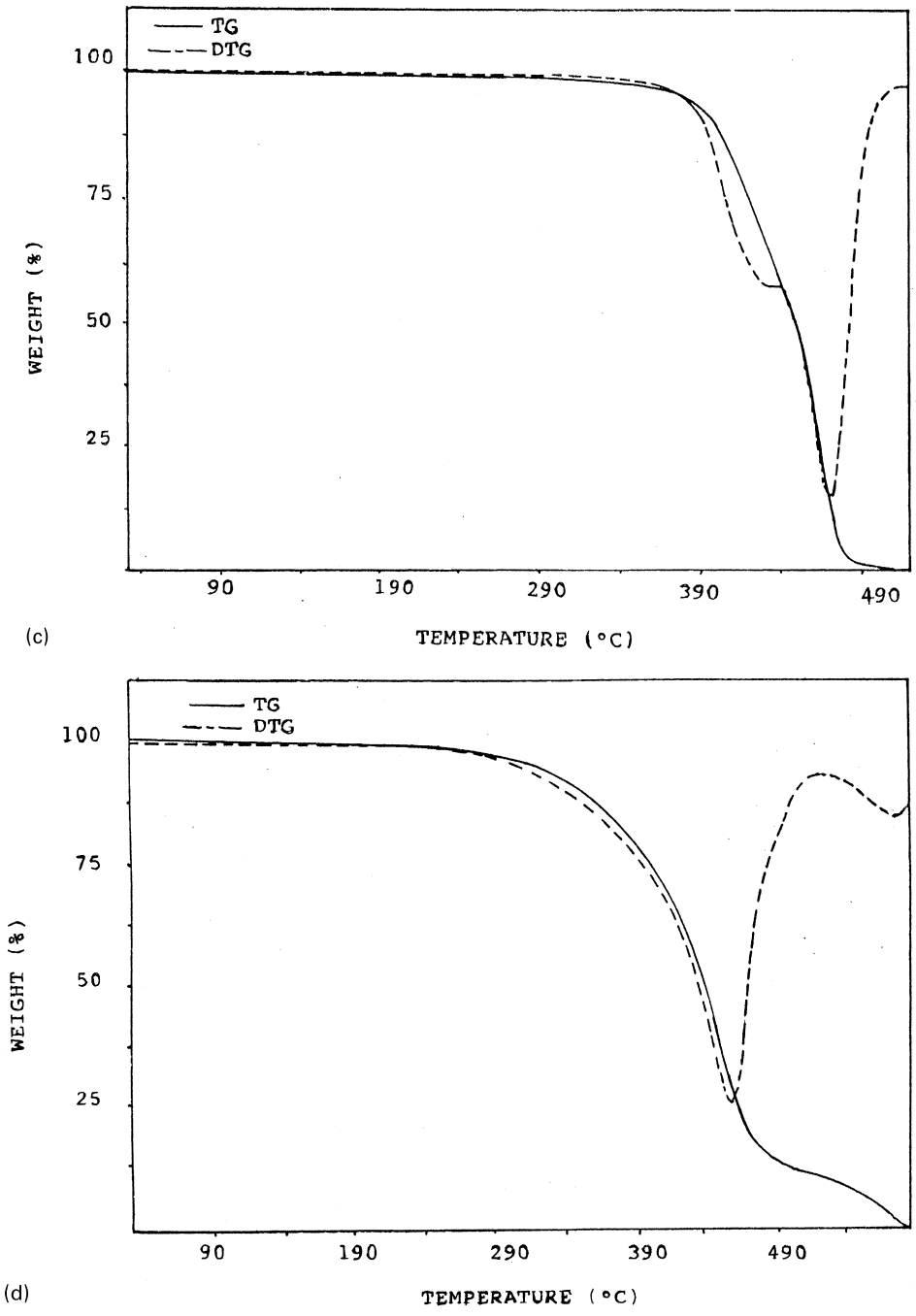

Fig. 2. (*continued*)

Maleic anhydride modified polypropylene (MA-PP) was prepared by melt mixing PP with maleic anhydride (five parts) benzoquinone (0.75 parts) and dicumyl peroxide (three parts) in a Brabender Plasticorder. The IR spectrum of the maleic anhydride modified polypropylene from which the unreacted maleic anhydride was extracted using acetone is shown in Fig. 1. The peak present at 1710 cm^{-1} indicates the presence of carbonyl groups originating from maleic anhydride grafted on PP. The phenolic modified polypropylene (Ph-PP) was prepared by melt mixing PP with dimethylol phenolic resin (SP-1045) (four parts) and stannous chloride (0.8 parts) at 180°C.

Blends of PP and NBR were prepared by melt mixing PP with NBR in a Brabender plasticorder (PLE-330) at a temperature of 180°C. The rotor speed was 60 rev min^{-1} and time of mixing 10 min. In compatibilised blends, the compatibiliser was added prior to the addition of NBR. The compatibiliser concentration was varied from 1 to 15 wt%. The dynamic vulcanisation of the blends was done by using three crosslinking agents, sulphur, peroxide and mixed system consisting of sulphur and peroxide. The formulation

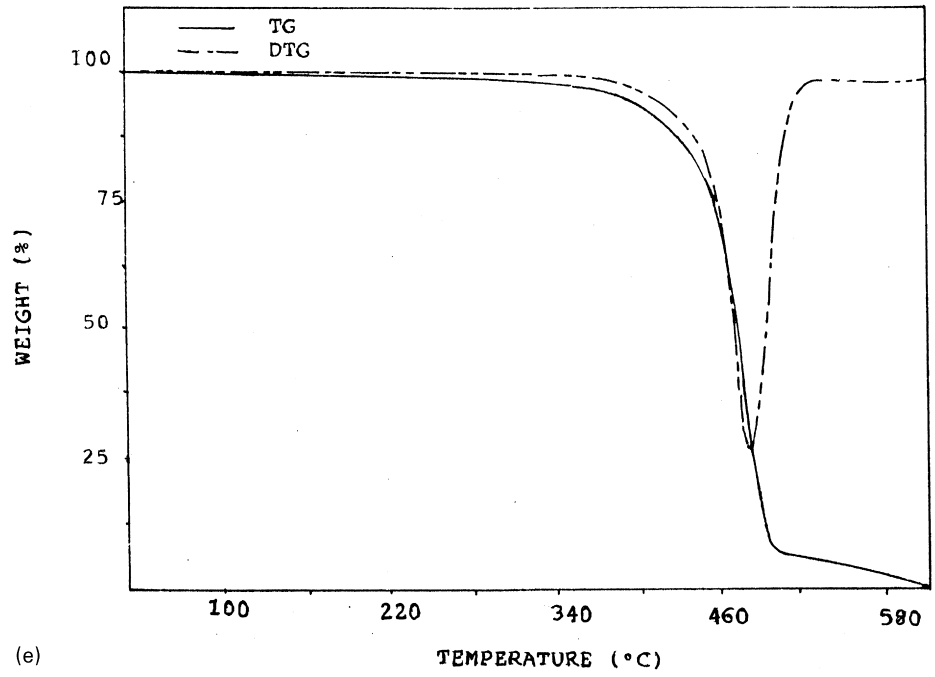

Fig. 2. (*continued*)

used is shown in Table 1. The binary blends were designated as P_{100}, P_{70}, P_{50}, P_{30} and P_0 where the subscripts denote the weight percentage of PP in the blend. The Ph-PP and MA-PP compatibilised P_{70} blends were designated as PP_{70x} and PM_{70x}, respectively, where x denotes the weight percentage of compatibiliser in the blend.

2.2. Thermogravimetric analysis

The thermogravimetry and derivative thermogravimetry were carried out in a Perkin–Elmer TGA7. The samples were scanned from 30 to 600°C at a heating rate of 10°C min^{-1} in nitrogen atmosphere.

2.3. Differential scanning calorimetry

The melting behaviour and crystallinity of PP/NBR blends were studied using a Perkin–Elmer DSC thermal analyser. The samples were scanned at a heating rate of 10°C min^{-1} in nitrogen atmosphere.

2.4. Wide angle X-ray scattering

The crystallisation behaviour of PP/NBR blends was analysed on a wide angle X-ray diffractometer using copper k_∞ radiation in the 2θ range of 5–30°.

2.5. Scanning electron microscopy

The morphology of the samples was analysed using scanning electron microscope. The samples for morphology measurement were prepared by cryogenically fracturing the samples in liquid nitrogen. The NBR phase was preferentially extracted from these samples using chloroform.

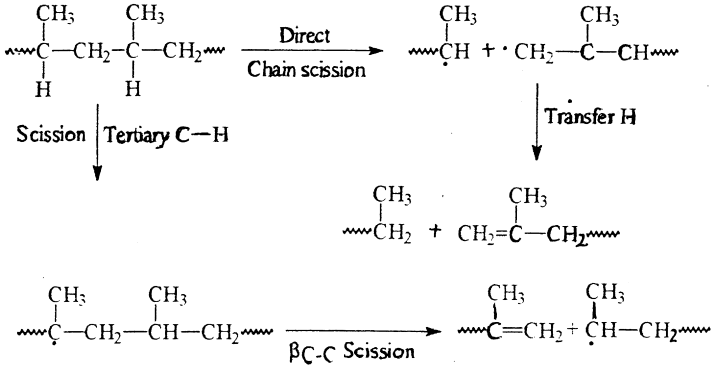

Fig. 3. Schematic representation of the mechanism of degradation of PP.

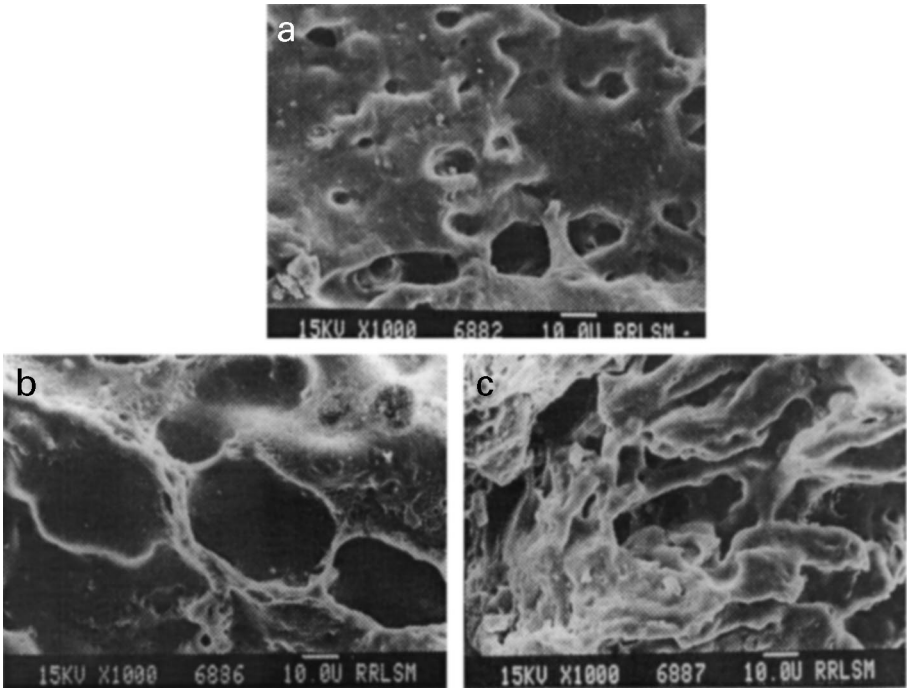

Fig. 4. Scanning electron micrographs of PP/NBR blends: (a) P_{70}; (b) P_{50}; and (c) P_{30}.

3. Results and discussion

3.1. Thermal degradation

Thermograms and derivative thermograms of pure PP, nitrile rubber and their blends are shown in Fig. 2a–e, respectively. In the case of PP, the weight loss is very low up to 250°C. Hence, the sample can be considered as stable up to this temperature in nitrogen atmosphere. The degradation of PP, which starts at 250°C was completed at 385°C. This weight loss in this region, 250–385°C, corresponds to the formation of volatile products which arise from the random chain scission and intermolecular transfer involving tertiary hydrogen abstractions from the polymer by the primary radical. The degradation products of PP involves monomer, 2-methyl-1-pentene, 2,4-dimethyl-1-heptene, 2pentene and isobutene. The mechanism of degradation of PP can be represented as shown in Fig. 3.

The degradation of nitrile rubber was in two stages. In the first stage, which starts at 414.7°C leads to a weight loss of 80.37% and completed at 526.76°C. In the next stage, the degradation started at 543.6°C and completed at 633°C with a weight loss of 11.86%. Hence nitrile rubber is stable up to 415°C. The two step weight loss in NBR was due to the degradation by the random chain scission of butadiene and acrylonitrile parts in NBR.

In the case of blends, the incorporation of NBR into PP was found to improve the thermal stability of PP. The incorporation of 30 wt% NBR increases the initial degradation temperature from 250 to 380°C, while further addition of NBR, i.e. at 50 wt% NBR, the initial degradation temperature shifts to lower side to 308°C. It is interesting to note that in P_{50}, the degradation was in two steps, while in P_{70} and P_{30} the degradation was in one step. This indicated the better interaction between PP and NBR in P_{70} and P_{30}. In the case of polymer blends, the thermal degradation depends on the morphology and extent of interaction between the phases. The morphology of PP/NBR blends are shown in Fig. 4. In P_{70} and P_{50} NBR is dispersed as domains in the continuous PP matrix and in P_{30}, NBR also forms a continuous phase along with the PP phase, resulting in a co-continuous morphology. As the weight percent of NBR increased from 30 to 50 wt%, the size of NBR domains increased from 5.87 to 18.7 μm. This increase in domain size at higher loadings of NBR is due to the coalescence of NBR domains. Hence, as the concentration of NBR is increased from 30 to 50 wt%, the interfacial area decreased and this reduced the extent of interaction between the phases. The interfacial area per unit volume of the blend for the blends was calculated using the following equation [33] :

$$A = n \times 4\pi R^2 \tag{1}$$

where A is the total area occupied by the dispersed phase, R the radius of the dispersed phase particle and n the number of particles of the minor phase per unit volume of the blend, which can be estimated from Eq. (2):

$$n = \frac{\phi_d}{4/3\pi R^3} \tag{2}$$

where ϕ_d is the volume fraction of the dispersed phase. The

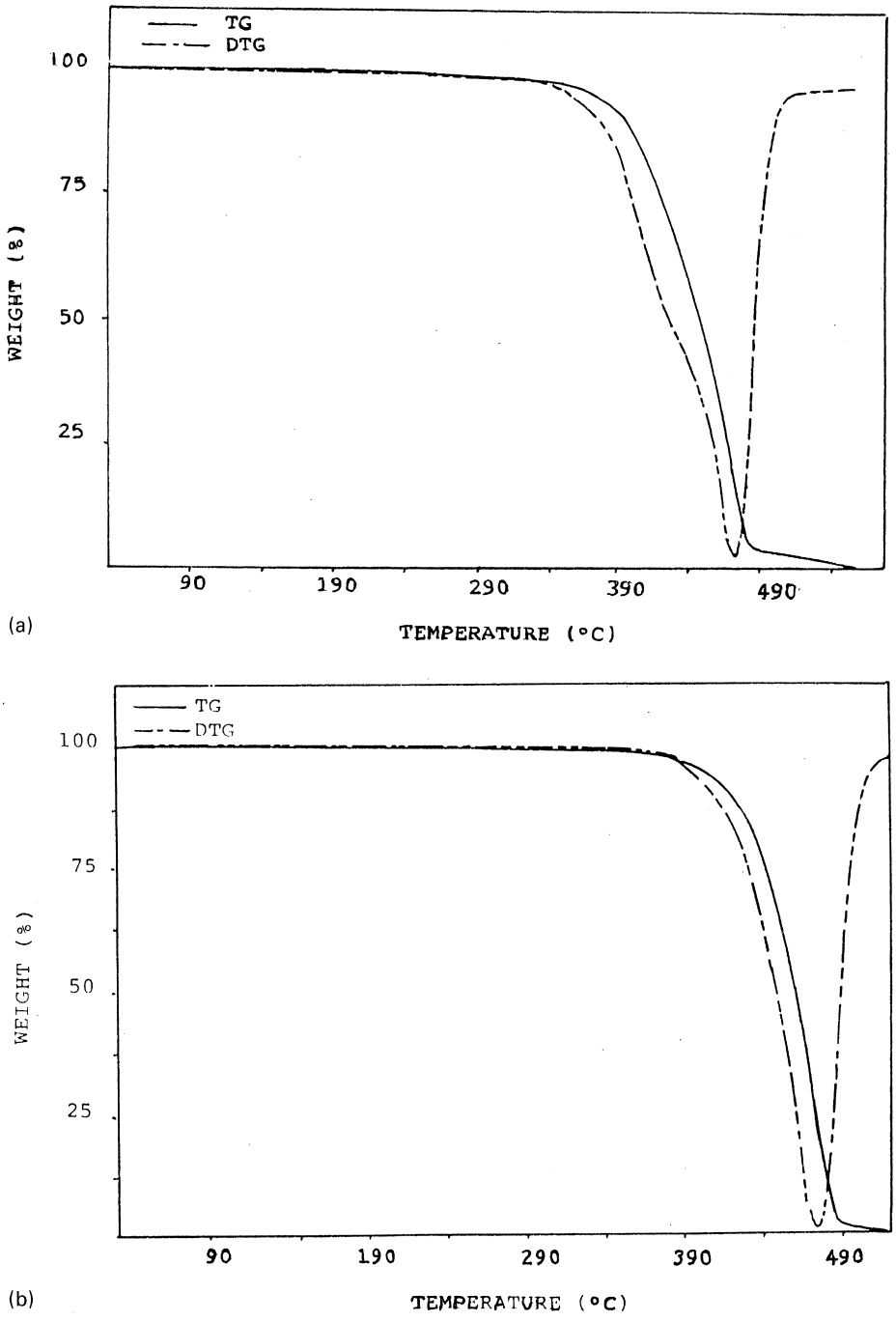

Fig. 5. Thermograms and derivative thermograms of Ph-PP compatibilised P_{70} blends: (a) $PP_{7007.5}$; and (b) PP_{7010}.

Table 2
Degradation temperature and weight loss of PP/NBR blends

	T_0 (°C)	$T_{degr.}$ (°C)	Total weight loss (%)	Weight loss at 300°C (%)	Weight loss at 400°C (%)	Activation energy (kJ mol^{-1})
P_{100}	250.81	353.33	97.85	16.67	100	24.82
P_{70}	380.36	472.61	93.89	1.04	10.07	42.33
P_{50}	308.29 520.51	460 575	93.84	2.08	25.69	24.8
P_{30}	382.7	480.87	89.62	1.38	6.94	66.14
P_0	415.71 543.65	480.93 577.21	92.23	1.38	3.82	58.81

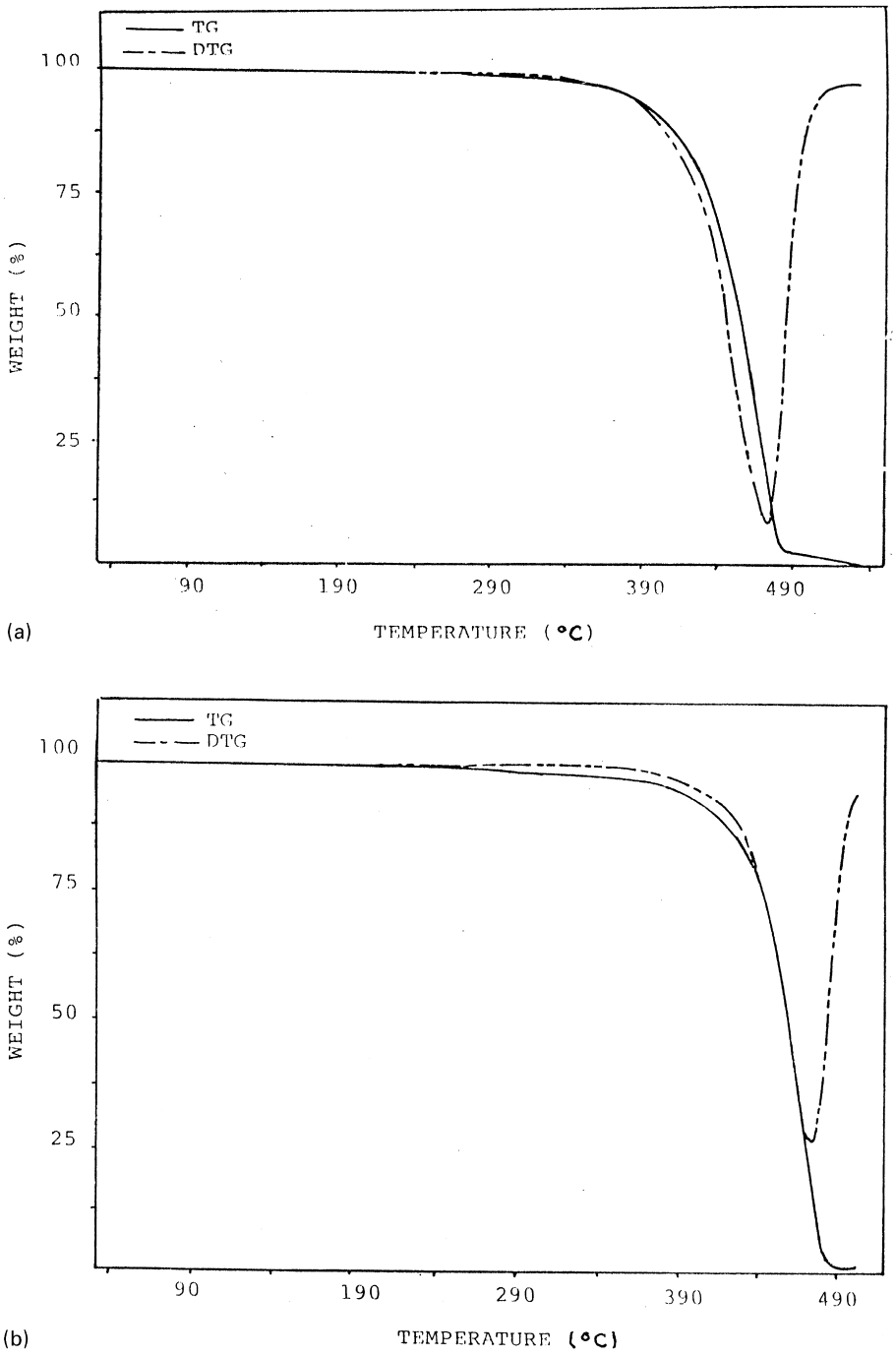

Fig. 6. Thermograms and derivative thermograms of MA-PP compatibilised P_{70} blends: (a) PM_{7005}; and (b) PM_{7010}.

Table 3
Thermal properties of compatibilised PP/NBR blends

	T_0 (°C)	$T_{degr.}$ (°C)	Total weight loss (%)	Weight loss at 300°C (%)	Weight loss at 400°C (%)	Activation energy (kJ mol^{-1})
P_{70}	380.4	472.6	93.89	10.07	98.6	42.33
$PP_{707.5}$	343.85	475.71	94.98	13.88	96.52	37.09
P_{7010}	380.36	475.86	96.18	6.25	98.61	53.67
PM_{7005}	364.17	474.09	94.33	10.42	97.92	46.05
PM_{7010}	380.36	474.32	94.32	7.64	98.61	51.06

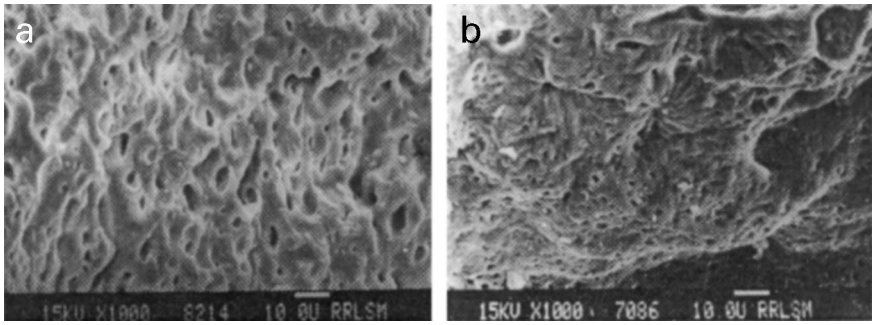

Fig. 7. Scanning electron micrographs of Ph-PP compatibilised blends: (a) $PP_{7007.5}$; and (b) PP_{7010}.

interfacial area per unit volume of the blend is decreased from 2.92×10^3 to 1.55×10^3 cm^2 on increasing the concentration of NBR from 30 to 50 wt%. The increased thermal stability of the blends, compared to PP may arise from the interaction of radicals formed during degradation of PP with nitrile rubber. Hence, the observed decrease in initial degradation temperature of P_{50} can be attributed to the decreased interaction between PP and NBR phases. At 70 wt% NBR, due to the co-continuous morphology, the possibility of interaction further increases and T_0 also showed an increase.

The degradation temperature corresponding to the main weight losses obtained from DTG curves are given in Table 2. The weight loss corresponding to different temperatures and the initial degradation temperature was also given in the table. The degradation temperatures of PP is at 353.33°C and that of NBR are at 480.93 and 577.2°C. The blends show intermediate values. Among the different blends, the P_{50} blend shows the lowest degradation temperature. The total weight loss and percentage loss at various temperatures of PP degradation was also decreased upon the incorporation of NBR.

3.2. Effect of compatibilisation

The thermograms and derivative thermograms of 70/30 PP/NBR blends compatibilised with phenolic modified PP and maleic anhydride modified PP are shown in Figs. 5a and b and 6a and b, respectively. The peak corresponding to the major weight loss in DTG curves are shifted to higher temperatures upon compatibilisation using both Ph-PP and MA-PP. Table 3 shows the degradation temperature and weight loss at different temperatures for the compatibilised blends. It can be seen from the table that the degradation temperature corresponding to the major weight loss increased on compatibilisation. The percentage weight loss at different temperatures decreased upon compatibilisation.

The improvement in degradation temperature on compatibilisation may arise from the better interactions between PP and NBR, which is evident from the micrographs given in Figs. 7 and 8 for Ph-PP and MA-PP compatibilised blends, respectively. From the micrographs, it is seen that the size of the dispersed NBR domains decreased as the addition of maleic anhydride modified PP. This is due to the dipolar interactions between the maleic anhydride groups of PP (Fig. 9) with polar NBR. In Ph-PP the compatibilising action arises from the graft copolymer formed between Ph-PP and NBR (Fig. 10), which will locate at the

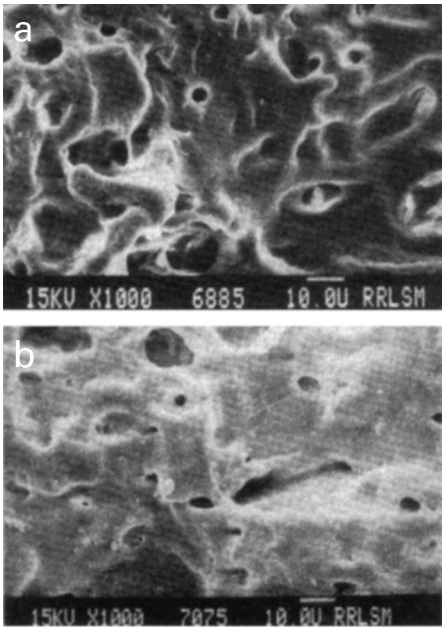

Fig. 8. Scanning electron micrographs of MA-PP compatibilised blends: (a) PM_{7005}; and (b) PM_{7010}.

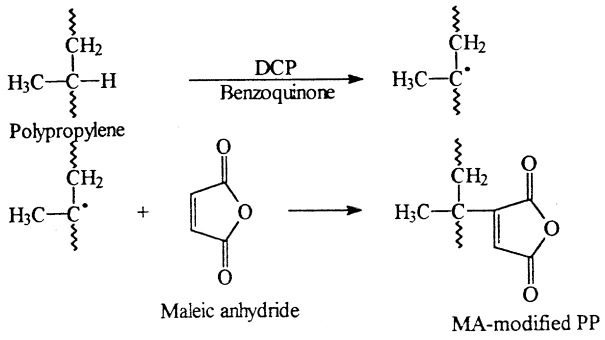

Fig. 9. Schematic representation of the maleic anhydride modification of PP.

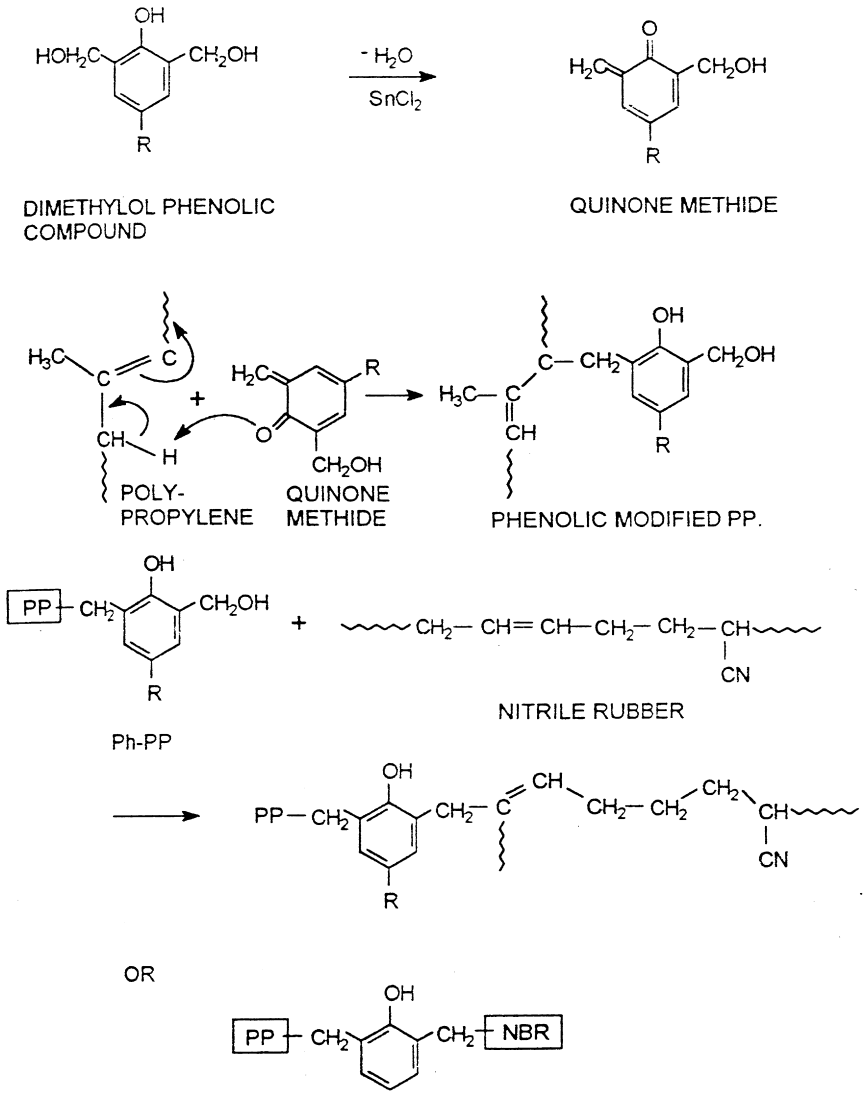

Fig. 10. Schematic representation of the dimethylol phenolic modification of PP and formation of graft copolymer between PP and NBR.

interface between PP and NBR phases. This will increase interfacial adhesion and interfacial area (Table 4) which leads to better interaction of radicals formed during degradation of PP and NBR. This type of improvement in degradation temperatures upon compatibilisation of immiscible polymer blends has been observed [34].

3.3. Effect of dynamic vulcanisation

The vulcanisation of rubbers, generally improve the degradation temperature since, more energy is required to break the bonds formed during vulcanisation. Figs. 11a–c show the thermograms and derivative thermograms of dynamic vulcanised P_{50} blends. The P_{50} blends were vulcanised using sulphur (PS), peroxide (PC) and a mixed system composed of sulphur and peroxide (PM). The data obtained from the thermograms and derivative thermograms are given in Table 5. From the table it is seen that, the initial degradation temperature T_0 is shifted to higher temperatures upon vulcanisation. The degradation temperatures corresponding to the two weight losses also show improvement upon vulcanisation. The initial degradation temperature is highest for mixed system crosslinked samples and the lowest for sulphur cured system. The peroxide cured system take an intermediate position, i.e. the degradation temperature follows the order PS < PC < PM.

Table 4
Interfacial area per unit volume in PP/NBR blends

Sample	Interfacial area $\times 10^{-3}$ ($cm^2\ cm^{-3}$)
P_{70}	2.92
$PP_{7007.5}$	8.66
PP_{7010}	12.04
PM_{7005}	4.58
PM_{7010}	4.40

Table 5
Thermal properties of dynamic vulcanised 50/50 PP/NBR blends

	T_0 (wt%)	$T_{degr.}$ (°C)	Total weight loss (%)	Weight loss at 300°C (%)	Weight loss at 400°C (%)	Activation energy (kJ mol^{-1})
PS-50	314.56 567.12	495.00 623.86	93.90	13.89	83.33	29.08
PC-50	324.7 552.2	483.47 596.95	93.62	19.44	84.03	22.85
PM-50	340.24 564.98	482.27 615.91	90.47	14.58	83.6	28.92

This behaviour can be explained by taking into consideration the type of crosslinks formed. The crosslinks formed during vulcanisation using different vulcanising systems are shown schematically in Fig. 12. In sulphur-cured system, the flexible and more heat sensitive mono or disulphidic linkages are formed, while in peroxide cured system, a more stable C–C linkages are formed. In mixed cured system, both –C–C– and –S_x– linkages are formed. Among the –C–C– and –S_x– linkages, more energy is required to break –C–C– linkages. Hence, the initial degradation temperature (T_0) is lowest for sulphur-cured system, which contains –S_x– linkages. At high temperatures, the PP undergoes depolymerisation in presence of DCP as shown below

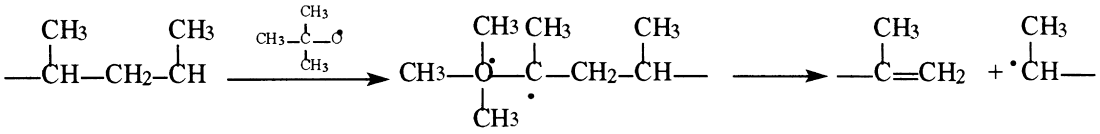

Hence, in peroxide and mixed cured system, the PP phase was degraded during vulcanisation. Since among PM and PC, the degradation must be more in the PC system with high DCP content, which in turn reduces the initial degradation temperature PC, though it contains more stable C–C linkages compared to PM.

The degradation temperatures corresponding to the two weight losses of the PS system are higher compared to the PM and PC systems. The lower degradation temperatures for PC and PM may be due to the degradation of PP, at the time of dynamic vulcanisation as explained earlier.

The activation energy for the degradation of the homopolymers and blends was determined using the Arrhenius equation,

$$\ln W = A - \frac{2.303E}{RT} \quad (3)$$

where W is the weight loss at a temperature T in Kelvin and E the activation energy. For the measurement of activation energy, the weight loss at different temperatures were considered so that the measured activation energy give a crude average over the energies at all the complex reactions occurring in the different materials at different temperatures. Among the blend compositions, the PP shows the lowest activation energy, and NBR the highest (Table 2), i.e. PP is more susceptible to degradation than NBR upon increasing temperature. The P_{50} blend shows the lowest activation energy among the blends, which also indicate the lowest interaction between PP and NBR in the blend.

In compatibilised blends, the activation energy increases which shows the better interaction (Table 3). However, on dynamic vulcanisation, the energy decreases for the peroxide-cured system. This indicates that the degradation of PP is enhanced in this system in presence of DCP (Table 4).

Table 6
Melting characteristics and crystallinity of PP/NBR blends

	T_{onset} (°C)	T_m (°C)	ΔH (cal g^{-1})
P_{100}	431.81	441.5	18.45
P_{90}	432.66	441.11	12.97
P_{70}	432.3	439.93	10.88
P_{50}	430.79	437.34	8.53
P_{30}	433.84	440.08	3.7

3.4. Differential scanning calorimetry

The melting behaviour of PP/NBR blends was analysed using DSC. The DSC traces of the binary blends are given in Fig. 13a–e The results obtained from the analysis of these traces are given in Table 6. From the table it is seen that the heat of fusion corresponding to the melting endotherm decreases upon the incorporation of NBR in to PP. The heat of fusion values depend on the crystallinity of the material. Hence, the crystallinity of these blends can be calculated from ΔH values as the ratio of the heat of fusion of the blend with that of the 100% crystalline PP (ΔHPP = 38 J g^{-1}). It can be seen from the table that the crystallinity of the system decreases with increase in the rubber content. This indicates that the crystallisation behaviour of the

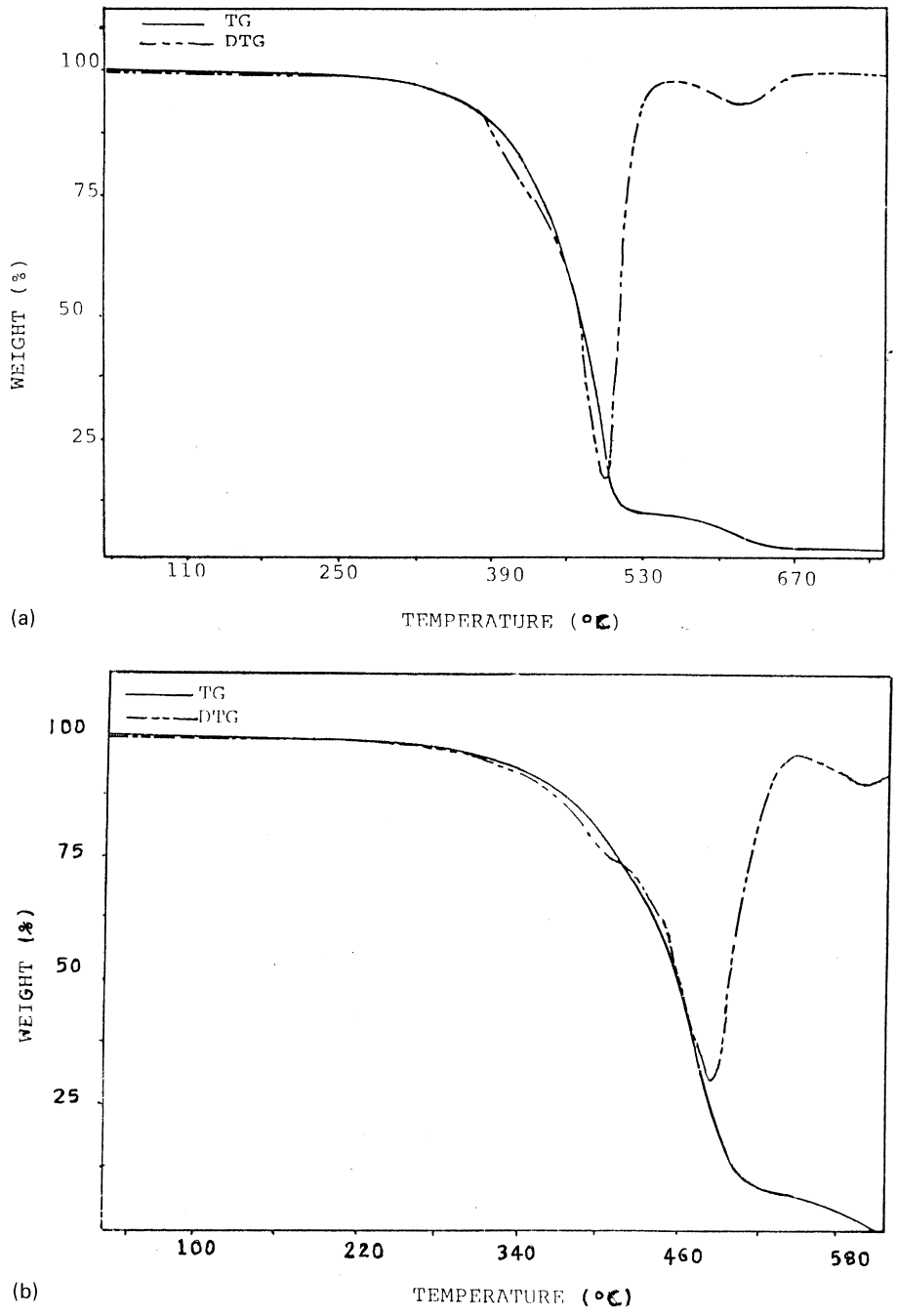

Fig. 11. Thermograms and derivative thermograms of dynamic vulcanised P_{70} blends: (a) PS; (b) PC; and (c) PM systems.

system was affected by the presence of nitrile rubber. Martuscelli et al. [18,19] have made detailed investigation on the effect of rubber phase on the crystallisation behaviour of thermoplastic elastomers, and observed that, the rubber particles are present in the inter and intra spherulitic region of the crystalline phase plastic. Hence the observed decrease in ΔH values and crystallinity (Fig. 14) is due to the fact that the formation of crystallites in the blend was affected by the presence of nitrile rubber. Again the melting temperature corresponding to the melting endotherm, also decreases upon the incorporation of rubber to PP. In the case of compatible blends, the decrease in melting temperature is related to the extent of interaction between the components according to Flory–Huggins theory [35]. However Stolp et al. [27] reported that, in the case of incompatible blends, the melting point decreased since the noncrystallisable component retard the crystal growth, which leads to unperfect crystals. Hence, the observed decrease in melting temperature on the addition of NBR is due to the impediment caused by NBR to the crystal growth of PP 3.5 wide angle X-ray scattering.

The properties of thermoplastic elastomers with a

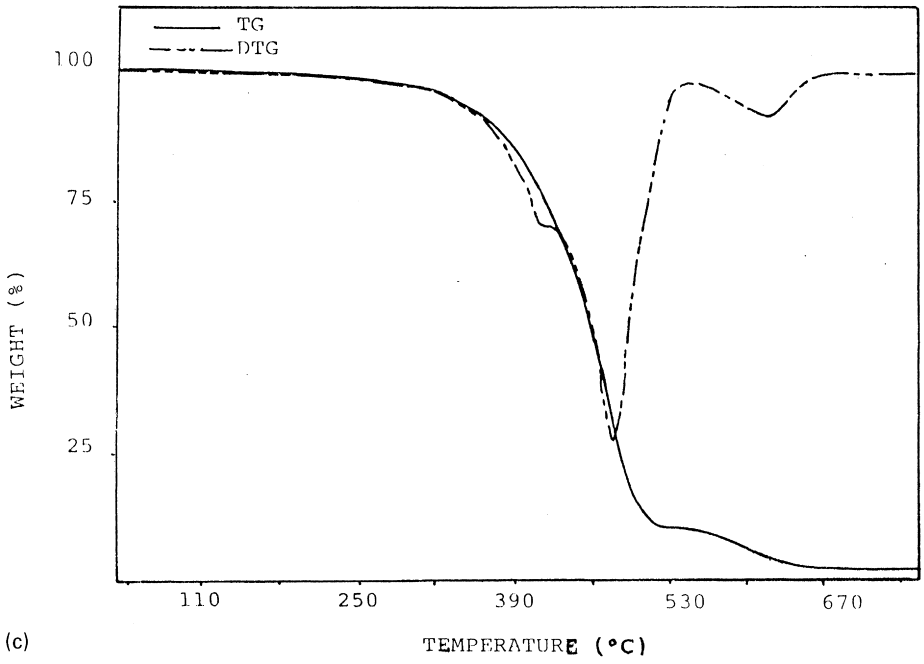

Fig. 11. (*continued*)

crystallisable component depends on crystalline structure, semicrystalline morphology and the crystallinity of the blends. The WAXS have been used to investigate the crystalline structure of PP/NBR blends. The X-ray diffractograms of binary PP/NBR blends are shown in Fig. 15. The isotactic PP generally has three types of crystalline structure α, β and γ forms depending on the crystallisation conditions. The WAXS spectrum of PP shows four maxima corresponding to the 110, 040, 130 and overlapping 131, 041 and 111 planes, which are characteristics of α-monoclinic structure at 2θ of 14.1, 16.8, 18.5 and 21.2°, respectively, in X-ray diffractograms. The incorporation of NBR into PP did not affect the crystalline structure of PP, i.e. the blends also exhibit the α-monoclinic structure. In PP, the highest intense peak is that at 2θ of 14.1°, however in the case of blends, the highest intense peak is that at 2θ of 16.8°. Table 6 shows the results obtained from the analysis of WAXD of PP and the binary blends. The addition of 30 wt%. NBR into PP increased the interplanar distance (*d* value). This indicates that rubber particles are present in the intra spherulitic structure of PP. As the concentration of NBR increased to 50 wt% and above the *d* value decreased. The decrease in *d* values at higher concentrations of NBR, may be due to the occlusion of rubber particles in inter spherulitic regions due to the large size of NBR at higher concentrations. In P_{30} also, the interplanar distance decreased than that of PP, which also indicates the absence of rubber phase in the spherulitic structure. The crystalline structure of PP/NBR blends is schematically represented in Fig. 16. The crystallinity of

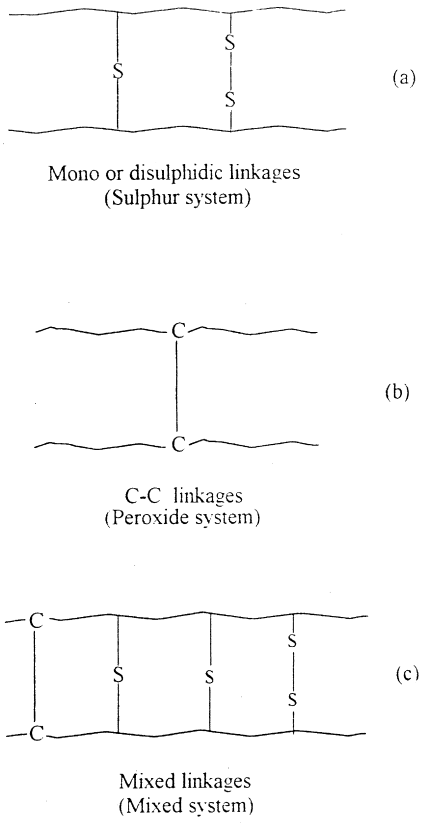

Fig. 12. Schematic representation of the different types of crosslinks formed during dynamic vulcanisation.

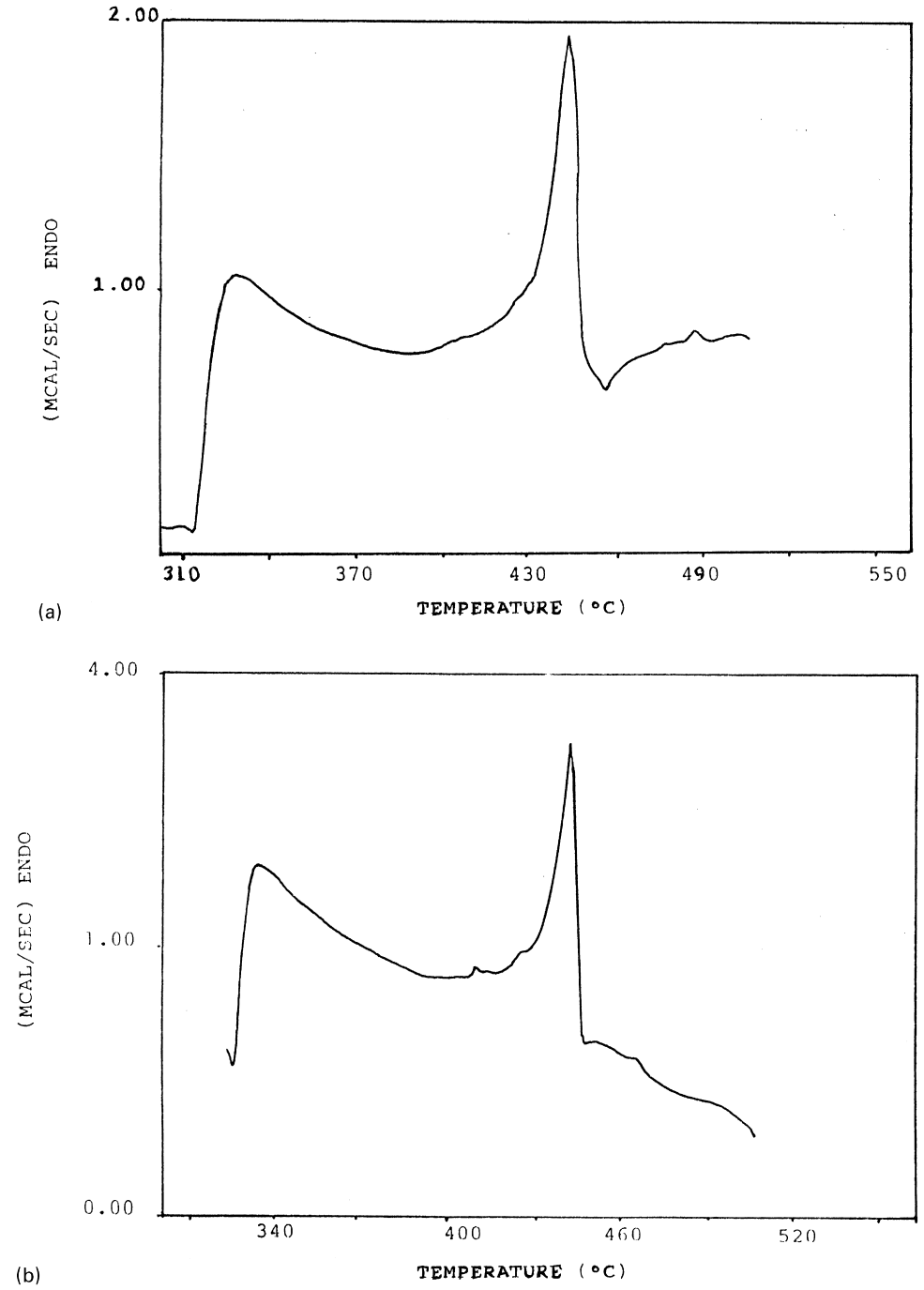

Fig. 13. Differential scanning calorimetric curves of PP/NBR blends: (a) P_{100}; (b) P_{90}; (c) P_{70}; (d) P_{50}; and (e) P_{30} blends.

Table 7
XRD data of PP/NBR blends

Reflection	P_{100}		P_{70}		P_{50}		P_{30}	
	2θ (°)	d (Å)	2θ (°)	d (Å)	2θ (°)	d (Å)	2θ (°)	d (Å)
110	14.05	6.30	13.99	6.33	14.04	6.31	14.08	6.29
040	16.85	5.26	16.77	5.29	16.85	5.26	17.09	5.19
130	18.52	4.79	18.5	4.79	18.50	4.79	18.66	4.75
111	21.22	4.18	21.68	4.09	21.14	4.21	21.53	4.13
% Crystallinity	54.23		53.26		40.17		32.9	

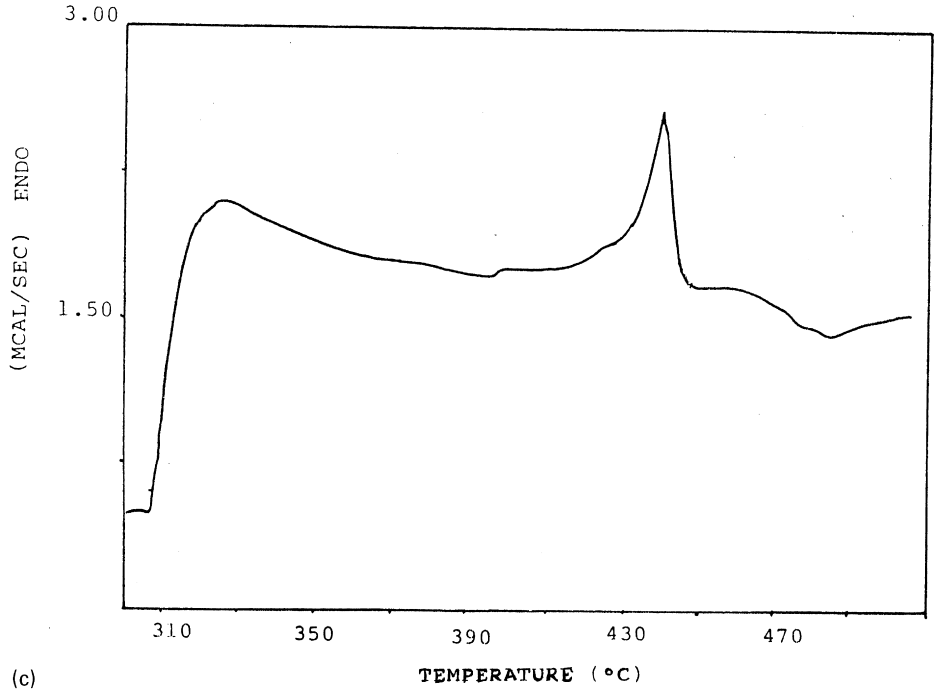

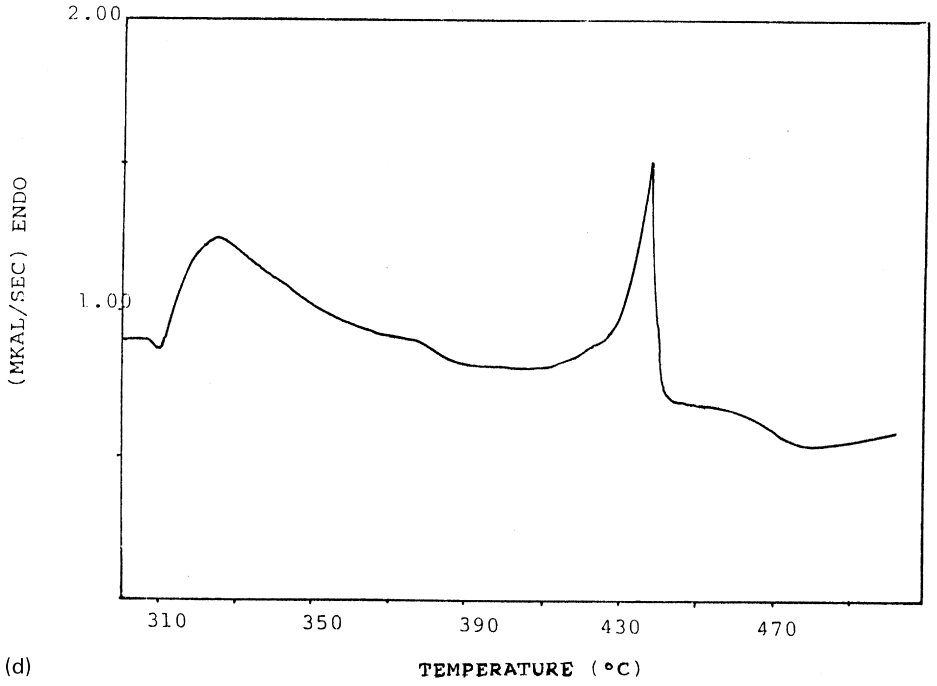

Fig. 13. (*continued*)

Table 8
XRD data of Ph-PP compatibilised 70/30 PP/NBR blends

Reflection	P_{7001}			P_{7005}			P_{7010}			P_{7015}		
	2θ (°)	d (Å)	L^a	2θ (°)	d (Å)	L^a	2θ (°)	d (Å)	L^a	2θ (°)	d (Å)	L^a
110	14.06	6.26	0.9	14.03	6.31	0.85	14.04	6.31	0.9	13.99	6.33	0.95
040	16.84	5.26	0.8	16.77	5.29	0.72	16.84	5.24	0.7	16.77	5.28	0.8
130	18.53	4.79	0.7	18.48	4.79	0.6	18.51	4.79	0.6	18.49	4.79	0.75
111	21.19	4.19	1.4	21.69	4.09	1.4	21.22	4.19	1.35	21.65	4.11	1.35

[a] The value of L is measured in arbitrary units.

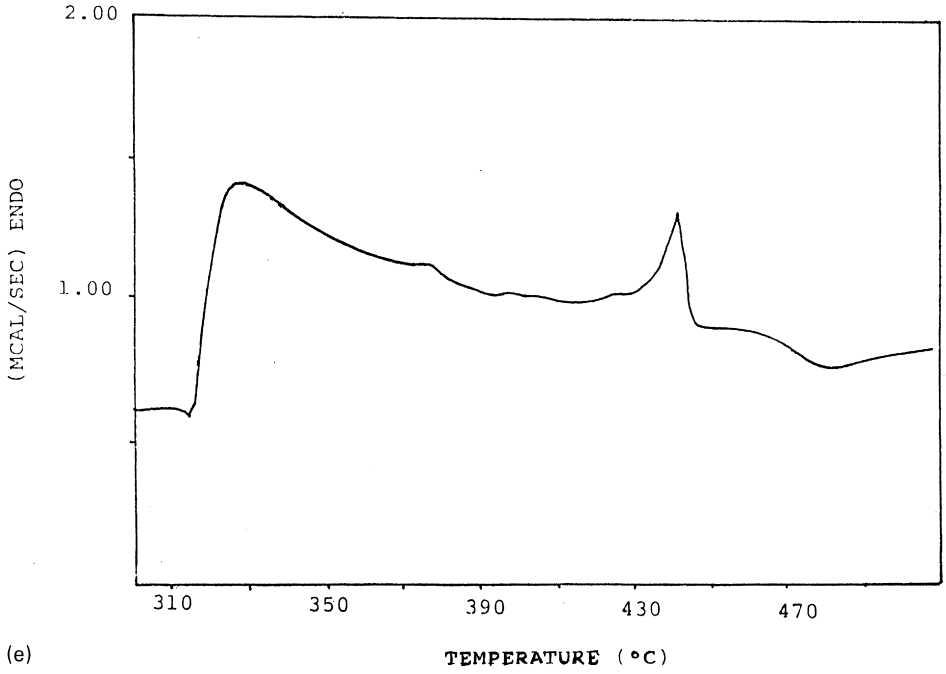

Fig. 13. (*continued*)

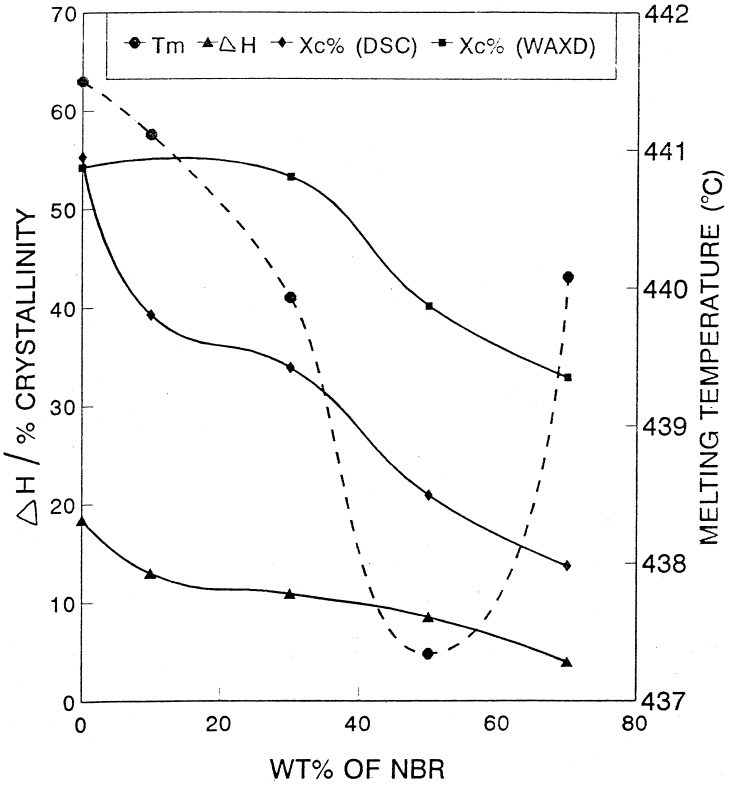

Fig. 14. Variation of crystallinity, ΔH and T_m with wt% of NBR.

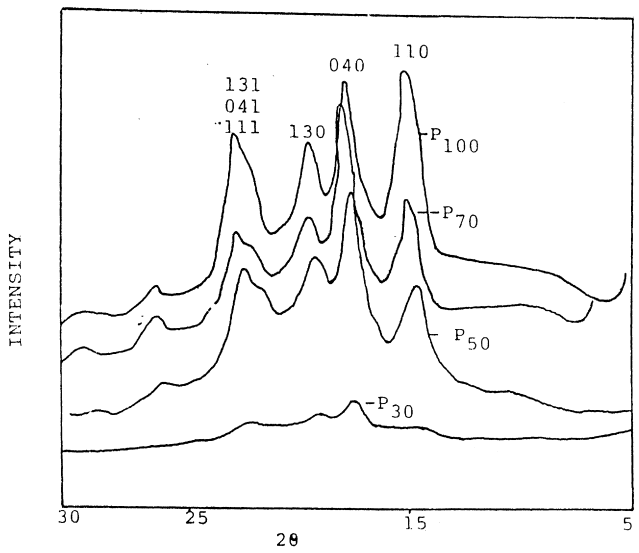

Fig. 15. Wide angle X-ray diffractograms of PP/NBR binary blends.

the blends was also calculated using Eq. (4).

$$X_c = \frac{I_c}{I_c + I_a} \quad (4)$$

where I_c and I_a are the integrated intensities corresponding to the crystalline and amorphous phases, respectively and X_c represents the degree of crystallinity. The results are given in Table 7. From the table it is seen that the values are higher than that obtained from DSC measurements.

The effect of compatibilisation of 70/30 PP/NBR blend (Table 8) with phenolic modified PP and maleic anhydride modified PP on the WAXD pattern is shown in Figs. 17 and 18. The compatibilisation in PP/NBR blends did not affect the α-monoclinic structure of PP. However, in literature it has been reported that the compatibilisation of the blends leads to a change in crystalline structure [23]. The data obtained from the WAXD patterns are given in Tables 8 and 9. From the table, it is seen that the compatibilisation of the blends using phenolic modified PP reduced the interplanar distance corresponding to different planes. The width at half height (L) for different reflections were also calculated, and it was observed that the peak width at half height which is the measure of spherulite size decreased upon compatibilisation. Hence, the size of spherulites increases upon compatibilisation since peak width at half height is inversely proportional to spherulite size. These observations indicate that on compatibilisation of PP/NBR blends using Ph-PP and MA-PP lead to a better crystallisation of PP component.

4. Conclusion

The thermal degradation of PP/nitrile rubber blends was investigated using the thermogravimetric method. The incorporation of nitrile rubber into PP improved the thermal properties of PP. The initial degradation temperature of PP was increased upon blending with nitrile rubber. Among the three blend compositions, the P_{50} blend showed the lowest degradation temperature. The thermal behaviour of various blend compositions was correlated with blend morphology. The weight loss corresponding to different temperatures was also decreased upon blending. The effect of compatibilisation of PP/NBR blend using phenolic modified PP and

Table 9
XRD data of MA-PP compatibilised 70/30 PP/NBR blends

Reflection	PM_{7001}		PM_{7005}		PM_{7010}		PM_{7015}	
	2θ (°C)	d (Å)	2θ (°C)	d (Å)	2θ (°C)	d (Å)	2θ (°C)	d (Å)
110	14.03	6.31	14.03	6.31	14.07	6.29	14.08	6.29
040	16.82	5.27	16.84	5.27	16.85	5.26	16.86	5.26
130	18.49	4.79	18.53	4.79	18.55	4.78	18.52	4.79
111	21.22	4.19	21.33	4.16	21.29	4.17	21.79	4.08

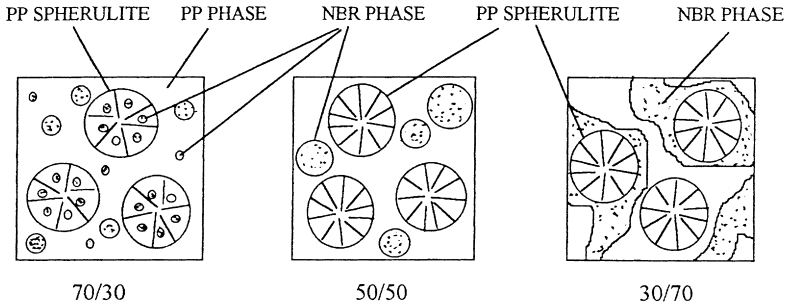

Fig. 16. Schematic representation of the crystalline structure of binary PP/NBR blends.

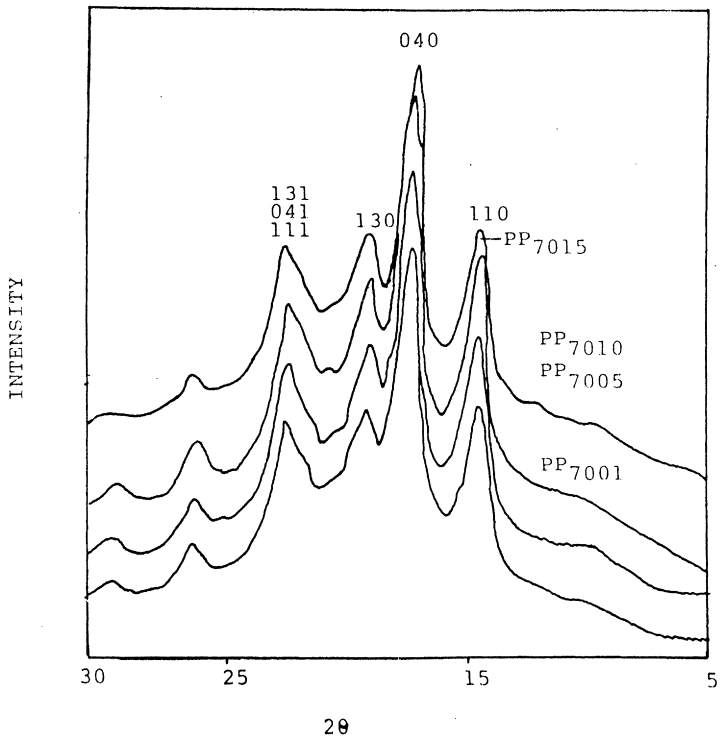

Fig. 17. Wide angle X-ray diffractograms of Ph-PP compatibilised P_{70} blends.

maleic anhydride modified PP on thermal degradation was also investigated. The compatibilisation increased the degradation temperature. The dynamic vulcanisation of the blends using sulphur, peroxide and mixed system consisting of sulphur and peroxide improved the thermal stability. Among the three vulcanised systems, the mixed vulcanised system showed the highest degradation temperature and sulphur-cured system showed the lowest

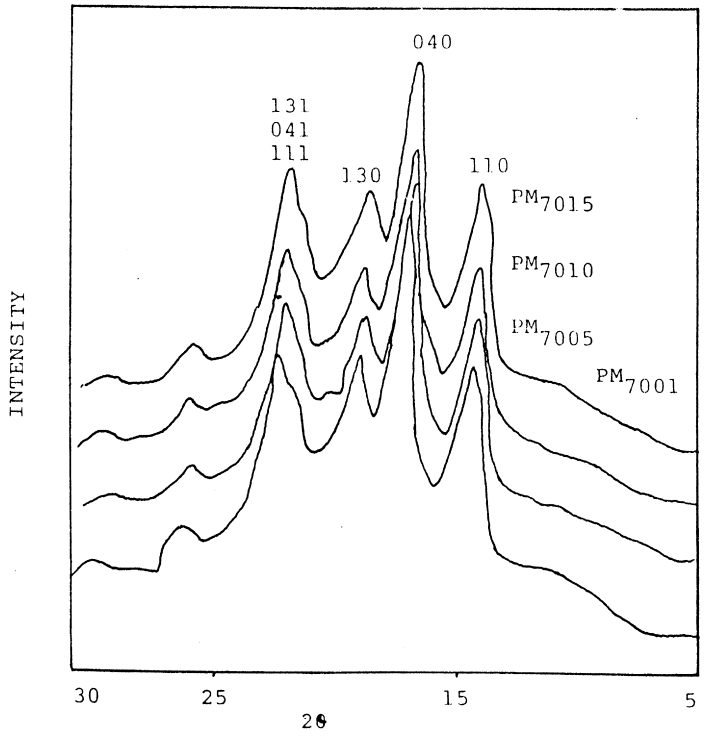

Fig. 18. Wide angle X-ray diffractograms of MA-PP compatibilised P_{70} blends.

value. The thermal behaviour of three types of dynamic vulcanised blends was correlated with the type of crosslinks formed. The melting behaviour of binary PP/NBR blends was also investigated using DSC. The melting temperature and heat of fusion values were decreased on the addition of NBR. The crystallinity of PP/NBR blends also decreased with increase in nitrile rubber concentration. The crystalline structure of PP/NBR blends was also investigated. The pure PP and the blends showed α-monoclinic structure as shown by the presence of four reflections corresponding to the four planes. The compatibilisation of the blends did not affect the α-monoclinic crystalline structure of PP. The incorporation of nitrile rubber into PP was found to increase the interplanar distance, which indicated the presence of rubber phase in intra spherulitic regions.

References

[1] Olabisi O, Robeson sLM, Shaw MT. Polymer–polymer miscibility. New York: Academic Press, 1978.
[2] Paul DR, Newman S, editors. Polymer blends New York: Academic Press, 1978.
[3] Xanthos M. Polym Engng Sci 1988;28:1392.
[4] Thomas S, Prud'homme RE. Polymer 1992;33:4260.
[5] Liao FS, Su AC, Tzu-chien X, Hsu J. J Polym 1994;35:2579.
[6] Inoue T, Suzuki T. J Appl Polym Sci 1995;56:1113.
[7] McNeill IC. In: Allen G, editor. Thermal degradation in comprehensive polymer science, 6. New York: Pregamon Press, 1989 chap. 15.
[8] Schnabel W. Polymer degradation principles and applications. New York: Hanser, 1981.
[9] Grassie N, editor. Developments in polymer degradation, 1–7. London: Applied Science, 1998.
[10] Varughese KT. Kaustschuk Gummi Kunststoffe 1988;41(11):114.
[11] Amraee IA, Kathab AA, Jollah SA. Rubber Chem Technol 1995;69:130.
[12] Lizymol PP, Thomas S. Polym Degrad Stab 1993;41:59.
[13] Subhra M, Mukunda PG, Nando GB. Polym Degrad Stab 1995;50:21.
[14] Chen C, Lai FS. Polym Engng Sci 1994;34:472.
[15] Lallandrelli L, Immirzi B, Malinconio M, Martuscelli E, Riva F. Makromol Chem 1992;193:669.
[16] Kang DK, Ha CS, Cho WJ. Eur Polym J 1992;28:6565.
[17] Martuscelli E. Thermoplastic elastomers from rubber–plastic blends. In: De SK, Bhowmick AK, editors. New York: Ellis Horwood, 1990.
[18] Martuscelli E, Silvlestre C, Abate G. Polymer 1982;23:229.
[19] Bartczak Z, Galeski ZA, Martuscelli E. Polym Engng Sci 1984;24:1155.
[20] Hlavata D, Plestil J, Zuchowksa D, Steller R. Polymer 1991;32:3313.
[21] Koshy AT, Kuriakose B, Thomas S, Varghese S. Polymer 1993;34:2438.
[22] Santra RN, Samantary BK, Bhowmick AK, Nando GB. J Appl Polym Sci 1993;49:1145.
[23] Wu CJ, Kuo JF, Chen CY. Polym Engng Sci 1993;33:1329.
[24] Inm DJ, Ha CS, Kim SC. Polymer (Korea) 1988;12:249.
[25] Ha CS. J Appl Polym Sci 1988;35:32.
[26] Choudhary NR, Chaki TK, Dutta A, Bhowmick AK. Polymer 1989;30:2047.
[27] Stolp M, Androsch R, Radusch HJ. Polym Networks Blends 1996;6:141.
[28] Horak Z, Krulis Z, Baldrain J, Fortenly I, Konecny D. Polym Networks Blends 1997;7:43.
[29] Coran AY, Patel R. Rubber Chem Technol 1983;560:1045.
[30] George S, Joseph R, Thomas S, Varughese KT. Polymer 1995;36:4405.
[31] George S, Neelakantan NR, Varughese KT, Thomas SJ. J Polym Sci B: Polym Phys 1997;35:2309.
[32] George S, Ramamurthy K, Anand JS, Groeninckx G, Varughese KT, Thomas S. Polymer 1999;40:4325.
[33] Matos M, Favis BD, Lomellini P. Polymer 1995;36:3899.
[34] Asaletha R, Kumaran MG, Thomas S. Polym Degrad Stab 1998;61:431.
[35] Flory PJ. Principles of polymer chemistry. New York: Cornell University Press, 1953.